Available online at www.sciencedirect.com
ScienceDirect
Fluid Phase Equilibria 251 (2007) 33–40
FLUID PHASE EQUILIBRIA
www.elsevier.com/locate/fluid

Liquid–liquid equilibrium of (1H,1H,7H-perfluoroheptan-1-ol + perfluoroalkane) binary mixtures

J.R. Trindade [a,b], A.M.A. Dias [a,1], M. Blesic [b], N. Pedrosa [a], L.P.N. Rebelo [b], L.F. Vega [c], J.A.P. Coutinho [a], I.M. Marrucho [a,*]

[a] *CICECO, Universidade de Aveiro, 3810-193 Aveiro, Portugal*
[b] *Instituto de Tecnologia Química e Biológica, ITQB2, Universidade Nova de Lisboa, Av. República, Apartado 127, 2780-901 Oeiras, Portugal*
[c] *Institut de Ciència de Materials de Barcelona, Consejo Superior de Investigaciones Científicas (ICMAB-CSIC), Campus de la U.A.B., 08193 Bellaterra, Barcelona, Spain*

Received 6 September 2006; received in revised form 26 October 2006; accepted 30 October 2006
Available online 7 November 2006

Abstract

This work presents new liquid–liquid equilibrium data for mixtures of 1H,1H,7H-perfluoroheptan-1-ol and linear perfluoroalkanes from C_6 to C_9. Data were measured at atmospheric pressure by turbidimetry and at pressures up to 5 MPa using a laser light scattering technique. The coexistence curves have been fitted to renormalization group extended-scaling expressions with the critical temperature and molar fraction obtained from the fit.

The soft-SAFT equation of state (EoS) was also used to describe the experimental data at both low and high pressures. A good description of the immiscibility gap was obtained with this approach although results seem to deteriorate at high pressures showing that the model cannot simultaneously describe the equilibrium and excess thermodynamic properties.

Keywords: 1H,1H,7H-perfluoroheptan-1-ol; Linear perfluoroalkanes; Liquid–liquid equilibrium; soft-SAFT EoS; Renormalization group theory

1. Introduction

Phase equilibrium studies of mixtures involving perfluoroalkanes are an actual and promising subject due to the important applications that these mixtures can find in a broad range of areas.

Extended attention has been given to perfluoroalkane (PFC) + alkane (HC) mixtures due to their use for industrial and environmental applications and also because of the unexpected non-ideal behaviour that these mixtures present. On the basis of the Scott and Hildebrand regular solution theory, these mixtures should be close to ideal, due to the small difference (ca. 1–2 $cal^{1/2}\,cm^{-3/2}$) of their solubility parameters that is insufficient to account for the characteristic incidence of liquid/liquid immiscibility in PFCs + HCs mixtures [1].

In previous publications [2,3] attention has been devoted to the measurement and modelling of vapou–liquid equilibrium (VLE) and liquid–liquid equilibrium (LLE) data for PFCs + HCs mixtures. These works and references therein, mention the unexpected immiscibility of these mixtures and the different attempts to justify this behaviour. The most accepted idea is that it is related with the weakness of the unlike forces governing the liquid mixture.

McLure et al. [1] studied the liquid–liquid co-existence curves of linear methylsiloxane-perfluoroalkane mixtures in order to study the influence of chain flexibility, where other effects as size and energy differences are also important. In this case, the difference in the solubility parameters is lower than in PFCs + HCs mixtures (ca. 1 $cal^{1/2}\,cm^{-3/2}$) although, as the authors noticed, dimethylsiloxane-perfluoroalkane mixtures actually exhibit positive deviations from ideality as large as those of the alkane-perfluoroalkane mixtures whose solubility parameter difference is larger. Following these studies, the LLE of mixtures of a perfluoroalcohol and linear perfluoroalkanes was measured and modelled and the results are presented in this work.

* Corresponding author. Tel.: +351 234 370200; fax: +351 234 380074.
E-mail address: imarrucho@dq.ua.pt (I.M. Marrucho).
[1] Present address: Departamento de Engenharia Biológica, Universidade do Minho, Campus de Gualtar, 4710-057 Braga, Portugal.

0378-3812/$ – see front matter © 2006 Elsevier B.V. All rights reserved.
doi:10.1016/j.fluid.2006.10.025

The importance of this study stems from both a practical and a fundamental point of view. The practical importance is justified by the considerable number of applications of perfluoroalcohols in a wide range of areas. Owing to their unique properties as high hydrogen bonding donor ability, low nucleophilicity, high ionising power and ability to solvate water, fluorinated alcohols have been used to allow reactions, which usually require the use of added reagents or metal catalysts to be carried out under neutral and mild conditions [4]. Another example is the "pseudo-hydroxide extraction", proposed as a method for separating alkali metal hydroxide from alkaline salt solutions using weakly acidic hydroxy compounds such as fluorinated alcohols. In both cases, the use of the fluoroalcohol facilitates the isolation of the products originating high yields, and the fluoroalcohols could be directly recovered from the reaction medium and reused. These processes bring an improvement from an environmental point of view, by suppression of effluents, in particular heavy metals, and they are particularly simple, since most of the reactions do not require any work-up [5].

Other recent applications of fluoroalcohols take advantage of their ability to originate and stabilize the formation of microemulsions for diverse medical and industrial applications [6,7] as well as their effect on protein conformations, notably the induction of α-helix formation. It was observed that the effectiveness of helix induction was found to increase exponentially with increasing number of fluorine atoms per alcohol molecule [8].

The hydrophobicity of such highly fluorinated molecules has also been used to polymerise an epoxy monomer in their presence with the aim of inducing a surface modification toward more hydrophobicity using cationic UV-curing as technique which is solvent free, giving high production rates and low energy requirements when compared to traditional polymerisation techniques [9].

However, it has also been recently reported that fluorinated telomer alcohols (FTOHs) may act as precursors to the perfluorinated acids (PFCAs) that have been detected widely in the environment as being ambient persistent and prejudicial for human beings [10]. Efficient techniques to recover these compounds before they react are also important from an environmental point of view.

From a theoretically point of view, this study can give new insights regarding the interactions between the constituents of the mixture helping to understand and develop accurate theoretical models to describe and predict the thermodynamic behaviour of this class of mixtures. Having in mind that the difference between the solubility parameters for the compounds studied in these mixtures is ca $2.6\,cal^{1/2}\,cm^{-3/2}$, higher than those mentioned before, it is interesting to test the soft-SAFT EoS in the description of these systems.

The experimental LLE data were measured by turbidimetry at atmospheric pressure and using a light scattering technique for higher pressures up to 4.5 MPa. Whenever possible comparisons with previously results for the alkane + perfluoroalkane mixtures [3] will be done, to conclude about the similarity of the thermodynamics of these two classes of mixtures.

The soft-SAFT EoS [11] was used to model the experimental data measured. The soft-SAFT EoS [11] was used to model the experimental data measured. This work appears as a continuation of previous publications [2,3,12] intending to characterize perfluoroalkanes and their mixtures with other classes of compounds using a versatile and robust EoS, in this case the *soft* version of the original SAFT EoS. The molecular parameters that characterize the pure perfluoroalcohol, according to the soft-SAFT model, were adjusted to densities and vapour pressures and are here presented. The molecular parameters of the PFC are taken from our previous work [2].

2. Experimental

Liquid–liquid equilibria of binary mixtures of 1H,1H,7H-perfluoroheptan-1-ol (CAS no. 335-99-9) + linear perfluoroalkanes, n-C_nF_{2n+2} (n = 6–9), were measured using synthetic methods: by turbidimetry at atmospheric pressure, and using a laser light scattering technique for measurements at pressures up to 5 MPa. 1H,1H,7H-perfluoroheptan-1-ol was obtained from Apollo Scientific with a purity of 98%. Perfluoro-*n*-hexane was bought from Sigma–Aldrich (99%), perfluoro-*n*-heptane from Apollo Scientific (98%) and both perfluoro-*n*-octane and perfluoro-*n*-nonane are from Fluorochem (99%). All the compounds were used without further purification. This decision was supported by the work of McLure et al. [1] who concluded that impurities in the mentioned range do not induce appreciable changes on the LLE data.

The experimental procedure applied was the same as previously used [3]. At a nominal pressure of 0.1 MPa, different samples of 1H,1H,7H-perfluoroheptan-1-ol + perfluoro-*n*-alkane were prepared in ampoules containing a magnetic stirrer. Samples with different compositions were prepared by weighting using an analytical high precision balance (±0.01 mg) model *Precisa 40 SM-200A*. The ampoules containing the mixtures at different compositions were then immersed in a thermostatic bath equipped with a calibrated Pt 100 temperature sensor with an uncertainty of 0.05 K connected to a multimeter, *Yokogawa 7561*. The water or alcohol thermostatic bath was sufficiently large to avoid temperature gradients. Cloud points were determined by visual observation by heating the samples until a homogeneous phase was obtained followed by slow cooling of the mixtures until phase separation was observed.

Measurements at pressure higher than the 0.1 MPa nominal pressure were obtained by a He–Ne laser light scattering technique. The fully automated apparatus [3] has a thick-walled Pyrex glass tube cell connected to a pressurization line and separated from it by a mercury plug. Scattered light intensity (I_{sc}) is captured at a very low angle ($2 < 2\theta\ (^\circ) < 4$) in the outer part of a bifurcated optical cable, while the transmitted light is captured in the inner portion of this cable. The cloud-point is the point on the $(I_{sc,corr})^{-1}$ against pressure (P) or temperature (T) least-squares fits where the slope changes abruptly. The cell can be operated in the isobaric or isothermal mode. Abrupt changes in either the transmitted or scattered light upon phase transition sharpen as the thermodynamic path approaches a perpendicular angle to the one-phase/two-phase surface. Temperature accuracy

is typically ±0.01 K in the range $240 < T\,(\mathrm{K}) < 400$. As for pressure, accuracy is ±0.01 MPa up to 5 MPa.

The density data for the 1H,1H,7H-perfluoroheptan-1-ol compound was measured with a vibrating tube Antón Paar DMA 4500 densimeter between 293.15 and 343.15 K at atmospheric pressure. The measuring principle is based on the calculation of the frequency of resonance of a mechanic oscillator with a given mass and volume, which is excited to be in resonance. The uncertainty of the measurements is $\pm 5 \times 10^{-4}\ \mathrm{g\,cm^{-3}}$. The vapour pressure data were taken from the literature [13]. These data were used to fit the molecular parameters for the soft-SAFT model [11] of this compound.

3. Modelling

3.1. Renormalization group theory

Systems with liquid–liquid equilibria present long-range concentration fluctuations in the vicinity of their consolute critical temperature. Asymptotically close to the critical point the thermodynamic properties vary as a simple power of the temperature difference or concentration difference with universal critical exponents, apart from a regular classical part. The non-classical behaviour of these systems as they approach their critical point is correctly taken into account from the renormalization group theory (RG) [14]. Since our experimental conditions were very close to the consolute critical temperature, we have used the RG theory [14] to correlate the experimental data and to obtain the critical temperatures and molar fractions of the studied systems. These properties are difficult to measure directly from experiments due to the extended flat critical region observed. According to the theory [15], asymptotically close to the critical point the thermodynamic properties vary as a simple power of the temperature difference or concentration difference (referred to their critical point values) with universal critical exponents and can be extended to describe the non-asymptotic region by the introduction of correction factors [16].

$$\Delta M = B_0 \tau^{\beta} \lfloor 1 + B_1 \tau^{\Delta_1} + B_2 \tau^{2\Delta_1} + \ldots \rfloor \tag{1}$$

where ΔM is the difference in the order parameter between the coexisting phases, β the critical exponent, B the amplitude, Δ_1 the correction exponent and $\tau = (T - T_c)/T_c$ holds for the reduced temperature that expresses the distance from the critical point. The order parameter is a quantity (mole fraction, volume fraction, density, etc.) chosen to measure the difference between the two coexisting phases.

By further considering the definition of the diameter of the coexisting curve [17] the following final equation is obtained:

$$x - x_c = fA\left(\frac{T - T_c}{T_c}\right)^{\beta} \tag{2}$$

where x stands for the molar fraction, being $f = 1$ for $x > x_c$ and $f = -1$ for $x < x_c$. A and β are parameters to be adjusted to the experimental data. In this work, we have used the mole fraction as the order parameter. This choice is usually guided by the symmetry of the equilibrium curves. The property that originates the most symmetric curves is usually chosen to be the order parameter.

3.2. Soft-SAFT model

The experimental data were also correlated with the soft-SAFT EoS [11]. The model was already used to study the vapour–liquid and liquid–liquid equilibrium data of mixtures of perfluoroalkanes both as a correlation and prediction method [2,3]. As usually done in SAFT-type equations, the soft-SAFT EoS is formulated in terms of the residual molar Helmholtz energy, A^{res}, defined as the molar Helmholtz energy of the fluid relative to that of an ideal gas at the same temperature and density. A^{res} is written as the sum of three contributions:

$$A^{\mathrm{res}} = A^{\mathrm{total}} - A^{\mathrm{ideal}} = A^{\mathrm{ref}} + A^{\mathrm{chain}} + A^{\mathrm{assoc}} \tag{3}$$

where A^{ref} accounts for the pairwise intermolecular interactions of the reference system, A^{chain}, evaluates the free energy due to the formation of a chain from units of the reference system, and A^{assoc}, takes into account the contribution due to site–site association. More details about the model for these particular systems can be found in references [11,17] and in the references therein.

The SAFT model describes a pure non-associating fluid as homonuclear chains composed of equal spherical segments bonded tangentially. Different fluids will have different number of segments, m, segment diameter, σ, and segment interaction energy, ε. The molecular parameters for the linear perfluoroalkane compounds had already been obtained and previously reported [2]. In this work, new molecular parameters are presented for 1H,1H,7H-perfluoroheptan-1-ol. The molecule was modelled as an associating compound with two associating sites that mimic the hydrogen bonds characterizing the perfluoroalcohol. These associating sites require two more molecular parameters to be considered, namely the energy and the volume of the associating site. For consistency with previous works, the associating parameters were chosen to be equal to those previously adjusted for normal alkanols, in a transferable manner [19].

When dealing with mixtures that are highly non-ideal, the Lorentz–Berthelot cross-interaction size and energy parameters need also to be adjusted to experimental data:

$$\sigma_{ij} = \eta_{ij}\frac{\sigma_{ii} + \sigma_{ij}}{2} \tag{4}$$

$$\varepsilon_{ij} = \xi_{ij}\sqrt{\varepsilon_{ii}\varepsilon_{jj}} \tag{5}$$

4. Results and discussion

Density data for 1H,1H,7H-perfluoroeptan-1-ol measured in this work is presented in Table 1. For the temperature range studied, experimental data were found to be correctly described by a linear equation of the type:

$$\rho_{\mathrm{calc}} = a - bT \tag{6}$$

where T is the temperature in K and ρ is the density in $\mathrm{g/cm^3}$. Coefficients for Eq. (6) are also reported in Table 1.

Table 1
Density data for the pure 1H,1H,7H-perfluoroheptan-1-ol and coefficients of $\rho_{calc} = a - bT$ with T in K and ρ in g/cm^3

T (K)	ρ (g cm^{-3})
Density	
293.15	1.7501
293.15	1.7502
303.15	1.7327
313.15	1.7150
323.15	1.6969
333.15	1.6785
343.15	1.6597
Coefficients	
a	2.2792
b	1.8033×10^{-3}
AAD	0.0004

Experimental LLE equilibrium data measured for the studied systems at atmospheric pressure and high pressure are reported in Tables 2 and 3, respectively. Experimental data at a nominal pressure of 0.1 MPa are presented in Fig. 1a and b in which compositions are expressed in terms of mole and volume fraction, respectively. Compositions in terms of volume fractions (ϕ) are calculated using the relation:

$$\phi_i = \frac{x_i}{x_i + K(1 - x_i)} \tag{7}$$

where $K = \rho_i M_j / \rho_j M_i$, being ρ and M the mass density and the molecular weight, respectively, of components i and j. It is interesting to remark that unlike most systems, the temperature versus composition diagrams of 1H,1H,7H-perfluoroheptan-1-ol + n-PFC mixtures are more symmetric when represented in terms of mole fractions than volume fractions. However, even in

Table 2
Experimental liquid–liquid solubility data for 1H,1H,7H-perfluoroheptan-1-ol (1) + n-perfluoroalkane (2) mixtures at atmospheric pressure

C_6F_{14}		C_7F_{16}		C_8F_{18}		C_9F_{20}	
T (K)	x_1	T (K)	x_1	T (K)	x_1	T (K)	x_1
1H,1H-perfluoro-1-heptanol+							
277.48	0.6649	275.97	0.7396	294.77	0.6991	299.15	0.7465
280.17	0.6314	280.44	0.7005	296.82	0.6710	305.75	0.6467
283.04	0.6012	285.53	0.6500	298.19	0.6483	307.42	0.5719
284.50	0.5753	289.23	0.5818	299.45	0.6265	307.92	0.5020
285.31	0.5591	287.42	0.6174	299.93	0.6058	307.93	0.4556
286.05	0.5388	284.38	0.6637	301.08	0.5582	307.78	0.4125
287.14	0.5050	281.61	0.6878	301.23	0.5427	307.74	0.3699
287.50	0.4874	277.35	0.7290	301.42	0.5264	305.71	0.2640
287.98	0.4579	289.50	0.5798	301.55	0.5087	304.86	0.2454
288.22	0.4339	290.88	0.5386	301.65	0.4864	303.49	0.2229
288.38	0.4026	291.47	0.5109	301.89	0.4113	302.36	0.2018
288.56	0.3536	292.07	0.4682	301.64	0.4838	298.05	0.1562
288.56	0.3094	292.10	0.4483	301.78	0.4596	295.11	0.1279
287.89	0.2291	292.15	0.4078	301.90	0.4397	271.97	0.8831
288.42	0.2857	292.18	0.3835	301.93	0.4256	279.07	0.8477
288.65	0.3429	292.15	0.3623	301.81	0.3779	291.22	0.8008
288.41	0.2959	292.15	0.3399	301.72	0.3380	297.11	0.7625
288.36	0.2568	291.95	0.2863	301.43	0.3068	301.97	0.7131
287.63	0.2167	291.89	0.2741	301.16	0.2933	304.83	0.6681
287.11	0.1900	291.20	0.2494	301.91	0.4135	306.86	0.6045
286.70	0.1716	292.20	0.3418	301.80	0.3643	307.93	0.5410
285.46	0.1495	292.20	0.3040	301.73	0.3478	301.03	0.1864
285.20	0.1419	291.52	0.2532	301.52	0.3205	306.26	0.2862
283.36	0.1265	291.18	0.2321	301.29	0.3027	306.80	0.3152
279.83	0.1066	290.37	0.2112	300.98	0.2840	307.33	0.3391
279.58	0.1026	289.35	0.1874	300.25	0.2539	286.03	0.0827
277.66	0.0919	288.18	0.1670	299.92	0.2449	292.73	0.1137
276.37	0.0877	286.94	0.1528	299.18	0.2246		
		285.59	0.1391	298.29	0.2060		
		283.71	0.1257	296.95	0.1836		
		278.03	0.0946	295.13	0.1650		
				287.11	0.7616		
				294.46	0.7033		
				293.19	0.7188		
				290.35	0.7403		
				279.03	0.8058		
				297.17	0.1889		
				294.57	0.1589		
				292.53	0.1416		
				290.65	0.1298		

Table 3
Experimental liquid–liquid solubility data for 1H,1H,7H-perfluoroheptan-1-ol (1) + *n*-perfluoroalkane (2) mixtures at pressures higher than atmospheric and resulting $(\partial T/\partial P)$ for distinct fixed compositions near the critical point

C_6F_{14} ($x_1 = 0.3710$)		C_7F_{16} ($x_1 = 0.3991$)		C_8F_{18} ($x_1 = 0.4277$)		C_9F_{20} ($x_1 = 0.4531$)	
P (MPa)	T (K)	P (MPa)	T (K)	P (MPa)	T (K)	P (MPa)	T (K)
1H,1H,7H-perfluoro-1-heptanol+							
0.589	288.75	0.542	291.99	0.179	301.78	0.226	307.97
0.630	288.75	0.890	292.02	0.535	301.82	0.594	308.03
0.822	288.73	1.273	292.04	1.071	301.89	1.160	308.14
1.066	288.73	2.011	292.10	1.585	301.95	1.746	308.25
1.560	288.70	2.523	292.14	2.304	302.04	2.171	308.33
2.185	288.67	3.240	292.19	2.757	302.08	2.821	308.45
2.234	288.67	3.825	292.24	3.077	302.12	3.339	308.54
2.647	288.64	4.450	292.28	3.721	302.20	3.819	308.62
3.282	288.61			4.150	302.26	4.406	308.73
3.984	288.58			4.425	302.30		
4.252	288.57						
$(\partial T/\partial P)_c \times 10^2$ (K MPa^{-1})							
−5.00		7.53		12.2		18.2	

terms of molar fraction the mixtures are less symmetric than the perfluoro-*n*-octane + *n*-alkanes measured previously as is also shown in Figure 1. The LLE equilibrium data for the mixture perfluoro-*n*-octane + *n*-octane measured in a previous work [3] is here used to elucidate about the difference in symmetry and immiscibility range characterizing each of these classes of mixtures.

The pressure dependence of the studied systems is given in Table 3. It was measured for a fixed composition near the critical point. Also given in Table 3 are the $(\partial T/\partial P)_c$ ratios calculated from the experimental data measured. It is important to mention that this ratio increases along the *n*-perfluoroalkane series studied passing from negative values for the mixture of the perfluoro-alcohol with C_6F_{14} to positive values for the other mixtures. This change in the signal of the pressure dependence derivative reflects a signal change in the excess volume. In fact, according to the Prigogine-Defay equation recently discussed by Rebelo et al. [20], near the critical region and under some restrictive assumptions [21], a Clapeyron-type of relationship can be established in which the pressure dependence of the critical temperature is directly related to the excess properties themselves,

$$\left(\frac{\mathrm{d}T}{\mathrm{d}p}\right)_x \cong T_c \frac{v^E(T_c(p), x)}{h^E(T_c(p), x)} \quad (8)$$

As a final comment on the symmetry of the coexistence curves, the experimental data were plotted as reduced T, defined as $T_{red} = T/T_c$, as a function of the molar fraction. The diagrams obtained are shown in Fig. 2 along with those for the perfluoro-*n*-octane + *n*-alkanes mixtures studied in a previous work [3]. It can be observed that a *global LLE diagram* can be visualized helping to support the universality theory reported by Munson [22] and Gilmour [23].

As mentioned in the previous section our experimental data at 0.1 MPa were correlated using relations derived from renormalization group (RG) theory. Eq. (2) was used to correlate our mutual solubility experimental data in the entire temperature interval, including the critical region. Values for A and β to be used in Eq. (2) together with the calculated values for the critical temperature, mole fraction and volume fraction for each mixture are reported in Table 4. The solid lines in Fig. 1a and b represent the correlations.

Fig. 3 presents the correlation obtained with the RG theory and the correlation given by the soft-SAFT EoS. As mentioned before, the molecular parameters for 1H,1H,7H-perfluoroheptan-1-ol were adjusted using the liquid density and vapour pressure data. The associative energy and volume parameters were chosen to be equal to the ones of a normal alcohols being equal to 3450 K and 2250 Å^3, respectively [18]. The remaining molecular parameters namely, the number of segments, m, segment diameter, σ, and segment interaction energy, ε, are 3.744, 4.245 Å and 252.7 K, respectively. Liquid densities and vapour pressures are fitted to experimental data with an AAD less than 0.08% and 0.6%, respectively.

In the case of the mixtures, the binary interaction parameters were adjusted to the experimental LLE data measured. A fixed size interaction binary parameter equal to 1.05 was used in a transferable way for all the mixtures. In this way, the energy interaction parameter was the only adjusted parameter and it was found to increase along the linear perfluoro-*n*-alkane series. Their values were equal to 0.9607, 0.9638, 0.9647 and 0.9655 from C_6 to C_9. In previous studies of LLE of mixtures with PFCs using the original soft-SAFT model [3] it was found that the EoS was not able to adequately describe the entire equilibrium diagram. It could provide an acceptable description of the

Table 4
Parameters to be used in Eq. (2) together with critical constants for the studied mixtures

System	A	β	ϕ_{1c}	x_{1c}	T_c (K)
$CF_2H(CF_2)_6H_2OH + C_6F_{14}$	0.6478	0.2510	0.380	0.371	288.36
$CF_2H(CF_2)_6H_2OH + C_7F_{16}$	0.8301	0.3144	0.349	0.399	292.31
$CF_2H(CF_2)_6H_2OH + C_8F_{18}$	0.8225	0.2963	0.326	0.428	301.81
$CF_2H(CF_2)_6H_2OH + C_9F_{20}$	0.7718	0.2749	0.304	0.453	307.73

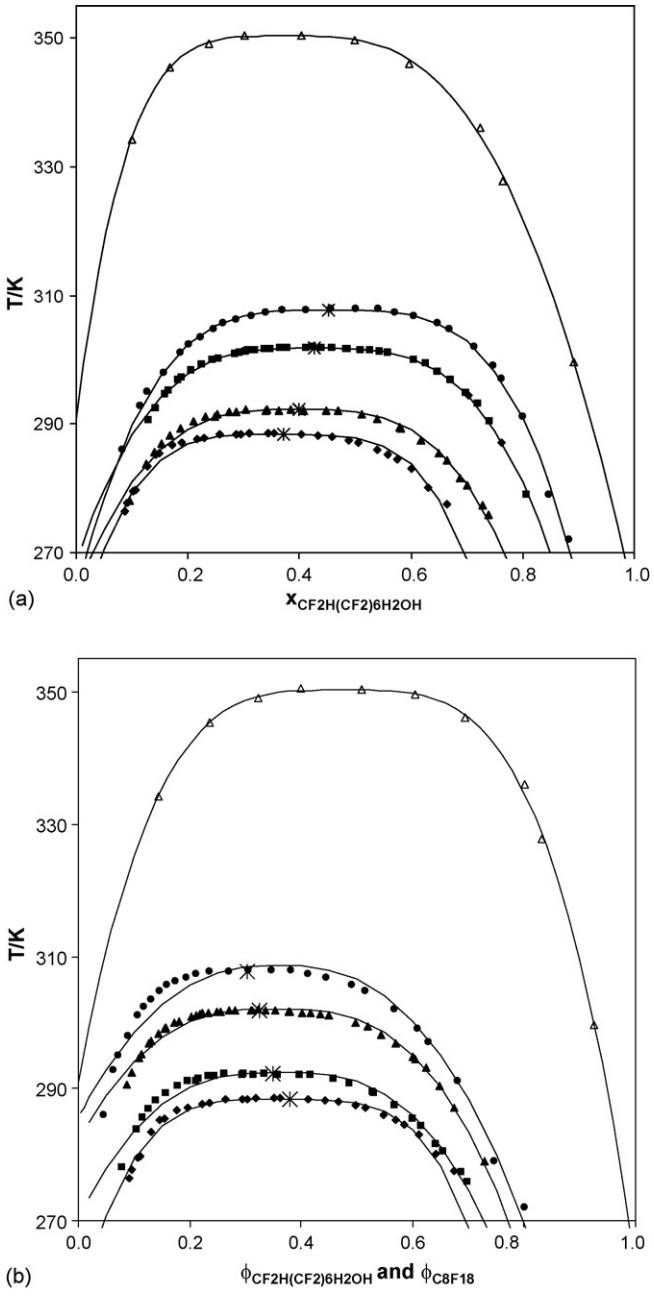

Fig. 1. Experimental and correlated coexisting curve of 1H,1H,7H-perfluoroheptan-1-ol + *n*-perfluoroalkanes (C_6–C_9) in terms of mole fraction (a) and volume fraction (b). Symbols represent solubility in *n*-hexane (♦), *n*-heptane (■), *n*-octane (▲) and *n*-nonane (●). Asterisk (*) represents the critical point for each mixture. The non-filled symbols represent data for *n*-octane + perfluoro-*n*-octane (△) measured by our group in a previous work [3]. The lines represent the correlated data calculated from renormalization group theory.

experimental data in the region far from the critical point and even the trend of the critical point shift with the alkane chain length change in the mixture, but it failed to describe the critical region. This is not the case for the mixtures studied in this work, where it was possible to accurately describe the LLE diagram both far and close to the critical point as shown in Fig. 3.

The binary interaction parameters adjusted using experimental data at 0.1 MPa have also been used to predict the pressure

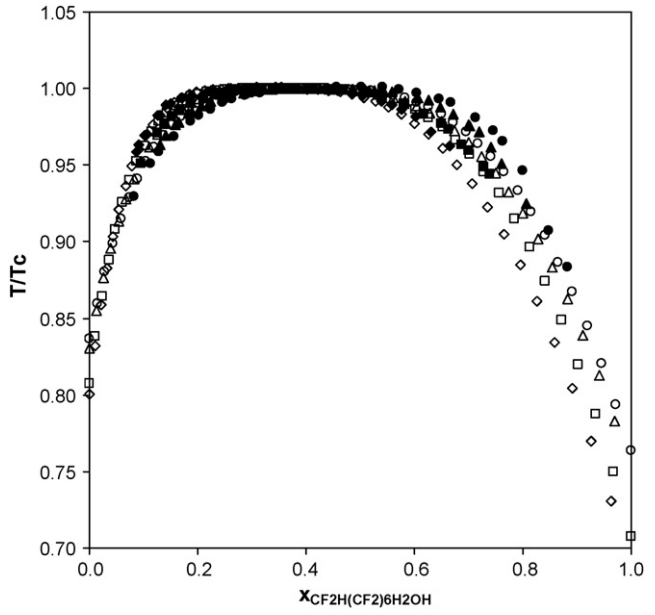

Fig. 2. Reduced temperature as a function of the molar fractions for all the mixtures studied in this work (full symbols) and also for perfluoro-*n*-octane + *n*-alkanes (non-filled symbols) using experimental data measured in a previous work [3]. Symbols as in Fig. 1.

dependence of the phase diagrams. However, these parameters were not capable of correctly describe the pressure dependence, being the theoretical predictions higher than the experimental ones as can be seen in Fig. 4. It was tried to fit binary parameters to the data measured at higher pressures to achieve an adequate representation of the pressure dependence of the phase diagrams.

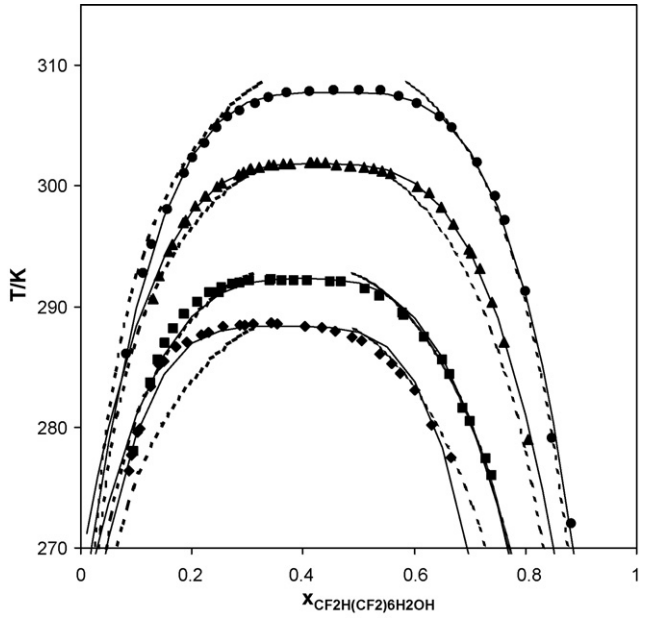

Fig. 3. Comparison between experimental LLE data for 1H,1H,7H-perfluoroheptan-1-ol + C_nF_{2n+2} mixtures at 0.1 MPa and the predictions obtained from the soft-SAFT EoS. Symbols represent the experimental data as in Fig. 1. The dashed lines represent the description obtained with soft-SAFT EoS when $\eta = 1.05$ and $\xi = 0.9607$, 0.9638, 0.9647 and 0.9655 from C_6 to C_9. The full lines represent the correlated data calculated from renormalization group theory.

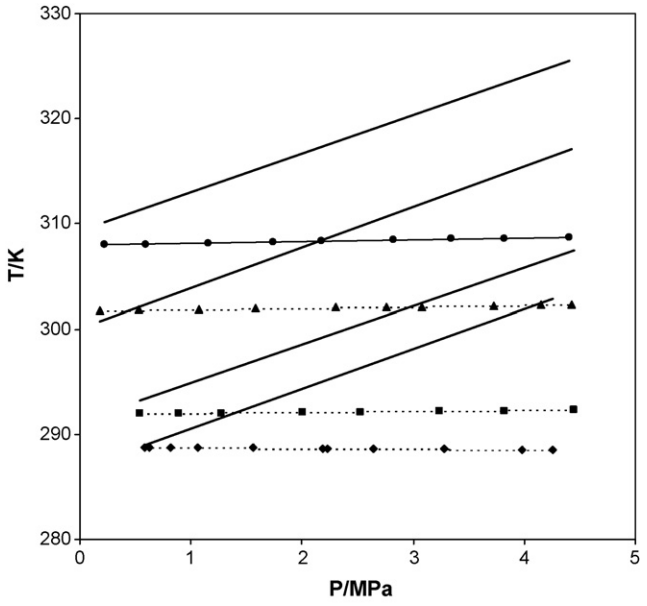

Fig. 4. Prediction of the high pressure experimental data obtained with the soft-SAFT EoS using the binary parameters adjusted for data at atmospheric pressure (full lines). Symbols as in Fig. 1 (with thinner lines being guides for the eye).

Nevertheless, using these parameters to describe the LLE data at 0.1 MPa, makes it possible to identify and locate the phase diagram on the composition scale but leads to an overprediction of the two phase region as expected from results reported in a previous work [3]. This shows that the soft-SAFT EoS is not able to simultaneously describe the g^E and the h^E and v^E. A good description of the g^E results in an accurate description of the phase diagram while a poor description of the h^E and/or v^E leads to a wrong pressure dependency of the critical point, according to Eq. (8). If one forces a good representation of the pressure dependence of the critical temperature, and hence, of the v^E/h^E ratio, a poor description of the phase diagram, and thus of g^E is obtained.

These results show that the soft-SAFT EoS, as it was presented in this work, cannot simultaneously describe the equilibrium properties (the LLE diagram) and the excess thermodynamic properties when using the same set of binary interaction parameters. Recent works presented derivations of two versions of the SAFT EoS, the soft-SAFT EoS [24] and the SAFT-VR Mie [25], and they are attempts to deal with situations as the one mentioned above. Both works, using different methodologies, intend to generalize the SAFT EoS in order to make it broad enough to be able to simultaneous describe equilibrium and excess properties, using a same set of parameters, that would also be more physically robust. In future work, it would be interesting to test the ability of these "extended versions" to predict the experimental data measured in this work.

5. Conclusions

In this work, liquid–liquid equilibria results of binary mixtures of 1H,1H,7H-perfluoroheptan-1-ol + perfluro-*n*-alkanes, *n*-C_nF_{2n+2} (n = 6–9), as measured by turbidimetry at atmospheric pressure, and using a laser light scattering technique, for measurements at pressures up to 5 MPa, are presented. A group renormalization theory was used to calculate the critical temperature and mole fraction for each mixture, which are difficult to observe experimentally due to the extended flatness of this region that these systems exhibit.

The soft-SAFT EoS was used to correlate the experimental data measured at atmospheric pressure. Using a fixed and transferable size binary interaction parameter, it was possible to accurately describe the equilibrium data measured including the critical region. The same binary interaction parameters proved to be inefficient to predict the higher pressure data measured. As future work, it would be interesting to look for the possibility of the existence of a set of molecular and/or interaction parameters that could simultaneously describe both equilibrium and excess data.

List of symbols

A	Helmholtz free energy
h^E	excess enthalpy
m	chain length (for Lennard-Jones segments)
M	molecular weight
ΔM	difference in the order parameter between the coexisting phases
p	pressure
T	temperature
v^E	excess volume
x	mole fraction

Greek letters

β	critical exponent
Δ_1	correction exponent
ε	segment interaction energy (between Lennard-Jones segments)
η	size parameter of the generalized Lorentz-Berthelot combination rules
ξ	energy parameter of the generalized Lorentz-Berthelot combination rules
ρ	mass density (kg m^3)
σ	size parameter of the intermolecular potential/diameter (for Lennard-Jones segments)
τ	reduced temperature that expresses the distance from the critical point
ϕ	volume fraction

Indices

c	critical
i	component
assoc	association term for soft-SAFT EoS
calc	calculated
chain	chain term for soft-SAFT EoS
ref	reference term for soft-SAFT EoS
res	residual term for soft-SAFT EoS

Acknowledgements

This project was financed by Fundação para a Ciência e Tecnologia, POCI/QUI/57716/2004. Partial support from the

Spanish government was provided under project CTQ2005-00296/PPQ.

References

[1] I.A. McLure, A. Mokhtari, J. Bowers, J. Chem. Soc., Faraday Trans. 93 (1997) 249–256.
[2] A.M.A. Dias, J.C. Pàmies, J.A.P. Coutinho, I.M. Marrucho, L.F. Vega, J. Phys. Chem. B 108 (2004) 1450–1457.
[3] M.J.P. Melo, A.M.A. Dias, M. Blesic, L.P.N. Rebelo, L.F. Vega, J.A.P. Coutinho, I.M. Marrucho, Fluid Phase Equilibr. 242 (2006) 210–219.
[4] J.P. Bégué, D. Bonnet-Delpon, B. Crousse, ChemInform (2004) 35–40.
[5] H. Kang, N.L. Engle, P.V. Bonnessen, L.H. Delmau, T.J. Haverlock, B.A. Moyer, Symposia Papers presented before the Division of Environmental Chemistry American Chemical Society, 2004.
[6] F. Giulieri, M.P. Krafft, Thin Solid Films 284/285 (1996) 195–199.
[7] A.N. Dobreva-Veleva, E.W. Kaler, K.V. Schubert, A.E. Feiring, W.B. Farnham, Langmuir 15 (1999) 4480–4485.
[8] N. Hirota, K. Mizuno, Y. Goto, J. Mol. Biol. 275 (1998) 365–378.
[9] M. Sangermano, R. Bongiovanni, A. Priola, D. Pospiech, J. Polym. Sci.: A: Polym. Chem. 43 (2005) 4144–4150.
[10] M.J. Dinglasan-Panlilio, S. Mabury, Environ. Sci. Technol. 40 (2006) 1447–1452.
[11] F.J. Blas, L.F. Vega, Mol. Phys. 92 (1997) 135–150.
[12] A.M.A. Dias, H. Carrier, J.L. Daridon, J.C. Pamies, L.F. Vega, J.A.P. Coutinho, I.M. Marrucho, Ind. Eng. Chem. Res. 45 (2006) 2341–2350.
[13] L.M.N.B.F. Santos, M.J.M. Monte, M. Fulhem, J.A.P. Coutinho, J. Chem. Eng. Data, submitted for publication.
[14] N. Nagarajan, A. Kumar, E.S.R. Gopal, S.C. Greer, J. Phys. Chem. 84 (1980) 2883–2887.
[15] J.M.H.L. Sengers, W.L. Greer, J.V. Sengers, J. Phys. Chem. Ref. Data 5 (1976) 1–52.
[16] F.J. Wegner, Phys. Rev. B 5 (1972) 4529–4533.
[17] M. LeyKoo, M.S. Green, Phys. Rev. A 16 (1977) 2483–2487.
[18] J.C. Pàmies, L.F. Vega, Ind. Eng. Chem. Res. 40 (2001) 2532–2543.
[19] J.C. Pàmies, Ph.D. Thesis, Universitat Rovira i Virgili, 2003.
[20] L.P.N. Rebelo, V. Najdanovic-Visak, Z.P. Visak, M. Nunes da Ponte, J. Trancoso, C.A. Cerdeiriňa, L. Romani, Phys. Chem. Chem. Phys. 4 (2002) 2251–2259.
[21] L.P.N. Rebelo, Phys. Chem. Chem. Phys. 1 (1999) 4277–4286.
[22] M.S.B. Munson, J. Phys. Chem. 68 (1964) 796–800.
[23] J.B. Gilmour, J.O. Zwicker, J. Katz, J. Phys. Chem. 71 (1967) 3259–3264.
[24] F. Llovell, C.J. Peters, L.F. Vega, Fluid Phase Equilibr. 248 (2006) 115–122.
[25] T. Lafitte, D. Bessieres, M.M. Pineiro, J.L. Daridon, J. Chem. Phys. 124 (2006).